Available online at www.sciencedirect.com
SCIENCE DIRECT
ELSEVIER
Materials Research Bulletin 41 (2006) 1430–1436
Materials Research Bulletin
www.elsevier.com/locate/matresbu

Hardness enhancement and oxidation resistance of nanocrystalline TiN/Mo_xC multilayer films

Q. Liu, X.P. Wang, F.J. Liang, J.X. Wang, Q.F. Fang *

Key Laboratory of Materials Physics, Institute of Solid State Physics, Chinese Academy of Sciences, POB 1129, 230031 Hefei, China

Received 25 August 2005; received in revised form 23 January 2006; accepted 11 February 2006
Available online 3 March 2006

Abstract

In this paper the influence of the layer's microstructure on the hardness enhancement in multilayer nanocrystalline films and the oxidation resistance are studied. The TiN/Mo_xC multilayer films at different modulation period, and Mo_xC and TiN monolayer films were deposited on the (0 0 1) silicon wafers and molybdenum sheets by rf and dc magnetron sputtering. The monolayer TiN films with a thickness of about 2 μm are of pure face-center cubic TiN phase, while the monolayer Mo_xC films consist of two phases, one of which is body-center cubic Mo and the other is hexagonal Mo_2C as determined by XRD. The coarse columnar grains of about 200 nm in the monolayer TiN films become much smaller or disappear in the multilayer films. The hardness enhancement of the multilayer films takes place at the modulation period of 320 nm, which can reach to 26 GPa and is much higher than the values of Mo_xC and TiN monolayer films. This enhancement in hardness can be explained as the decrease in the size and/or disappearance of columnar grains in the TiN layer. The Young's modulus in the temperature range from 100 to 400 °C increases with decreasing modulation period. It is found that about 100 nm thick TiN films can increase largely the oxidation resistance of Mo_xC films.
© 2006 Elsevier Ltd. All rights reserved.

PACS: 68.60.Bs; 81.15.Cd; 81.05.Je

Keyword: B. Sputtering

1. Introduction

In recent years multilayer films have attracted researchers' attention due to the prominent properties contrast to monolayer films in many aspects, such as oxidation resistance [1–3], wear resistance [4,5], and high hardness and fracture toughness. Some explanations about the property enhancement of the multilayer films have been proposed, such as (1) Hall–Petch-like model and Orowan model that consider the process of dislocation generation and motion in the multilayer films [6,7]; (2) the supermodulus effect model [8], which explains the hardness enhancement of materials by the supermodulus effect on the line tension of dislocation; (3) the coherent strain model [9,10]; (4) the elastic modulus difference model [11,12]. Among these explanations, the mechanism that the dislocations generated within one layer are blocked by the interface between layers is widely accepted for the hardness enhancement. These studies, however, mainly stay in the modulation period (designated as Λ and defined as the sum of the thickness of the two adjacent layers) below 100 nm. For $\Lambda > 100$ nm where the superlattice effects are indistinct, few works

* Corresponding author. Tel.: +86 551 5591459; fax: +86 551 5591434.
E-mail address: qffang@issp.ac.cn (Q.F. Fang).

0025-5408/$ – see front matter © 2006 Elsevier Ltd. All rights reserved.
doi:10.1016/j.materresbull.2006.02.008

about the properties of multilayer films have been done. There are still open questions on the origin of anomaly enhancement of the mechanical properties of multilayer films, for example, the influence of layer structure. If the layers in multilayer films are polycrystalline, not only the interfaces between the two layers, but also the grain boundaries or interfaces within the layer, could affect the properties of the multilayer films.

Titanium nitride (TiN) has been widely used in protective coatings for bearings, gears, and cutting tools due to its good wear resistance and inertness to steels. However, TiN coatings predominantly grow with a columnar grain structure. These columnar grain boundaries become the sites for crack initiation, resulting in premature failure of TiN coatings [13]. Therefore, the columnar structure of TiN coatings should be eliminated. There are at least two ways to maintain a fine equiaxed microstructure throughout the coating thickness, one of which is to deposit nano-composite films where the nano-crystallite TiN disperses uniformly in an amorphous matrix [14], and the other is to prepare multilayer films in which the growth of TiN is periodically interrupted by introducing nanolayers of a different material to force TiN to renucleate [15]. Molybdenum carbide was usually used as catalysts instead of hard coatings because of the low oxidation resistance, although hardness as high as 18 GPa was reported in MoC coatings [16,17]. Therefore, it is of great interest to improve the oxidation resistance of MoC coatings.

In this paper, TiN/Mo_xC multilayer films with different modulation periods Λ prepared by rf and dc magnetron sputtering, and their microstructure and properties such as hardness, Young's modulus, and oxidation resistance were investigated, in aims to reveal the influence of interfaces between layers and within the layer, and to improve the oxidation resistance of Mo_xC in virtue of the high oxidation resistance of TiN.

2. Experimental

TiN/Mo_xC multilayer films, TiN and Mo_xC monolayer films were deposited in a magnetron sputtering instrument equipped with rf and dc cathodes. The composite target for deposition of Mo_xC was made from pure graphite (99.8%) and molybdenum (99.99%) [18], while the target for deposition of TiN was the pure titanium (99.99%). The composite target of Mo_xC and the Ti target with a diameter of 60 mm were mounted on the rf and dc cathodes, respectively. The distance between the targets and the substrate is fixed as 60 mm. The TiN/Mo_xC multilayer films were fabricated by alternatively depositing Mo_xC and TiN at different modulation periods on the (0 0 1) Si wafers or molybdenum sheets in a size of 40 mm $\times$ 5 mm $\times$ 0.14 mm. The Si and Mo substrates were polished on the polishing machine, ultrasonically cleaned in a mixture of acetone and alcohol, rinsed in de-ionized water, dried in a nitrogen jet, and then introduced into the chamber immediately. The deposition chamber was pumped to 8×10^{-4} Pa before deposition. Argon was employed as sputtering gas and nitrogen was introduced into the chamber as reacting gas only in the period of TiN layer deposition. The pressure ratio between argon and nitrogen gas is 2:1 with a total working pressure of 1 Pa. The temperature of the substrate is kept as 400 °C during the whole deposition process.

The cross-section morphology and thickness of the films were investigated using field emission scanning electron microscopy (FESEM, Sirion 200, FEI). The hardness values were measured by a nanoindenter system at room temperature. The phase composition and microstructure were revealed by XRD measurement with Cu Kα radiation (Philips X'pert PRO MPD). The Young's modulus and the internal friction of films on Mo substrate were measured with the vibration reed instrument built in our laboratory [19], and the oxidation resistance of these films was tested with a thermo-gravimetric analyzer (Pyris 1 TGA).

3. Results and discussion

3.1. Microstructure

The XRD spectra of all samples are shown in Fig. 1, where the spectrum of Si substrate is also shown for comparison. In the monolayer TiN film deposited by dc sputtering a pure face-center cubic TiN phase is obtained. The ratio between the intensity of peaks (1 1 1) and (2 0 0) is relatively large, which indicates a texture on the (1 1 1) direction and is consistent with the columnar structure illustrated in the next section. The grain size of crystalline TiN is about 90 nm in the monolayer film, as estimated from the peak width by Debye–Scherrer equation after subtraction of instrumental broadening and listed in Table 1. The XRD pattern of monolayer Mo_xC films can be indexed by two phases, that is, the body-center cubic molybdenum and the hexagonal Mo_2C. The grain size of Mo and Mo_2C is about 20 nm as listed in Table 1. The existence of excess Mo, together with the fact that the Mo_2C can crystallize easily even

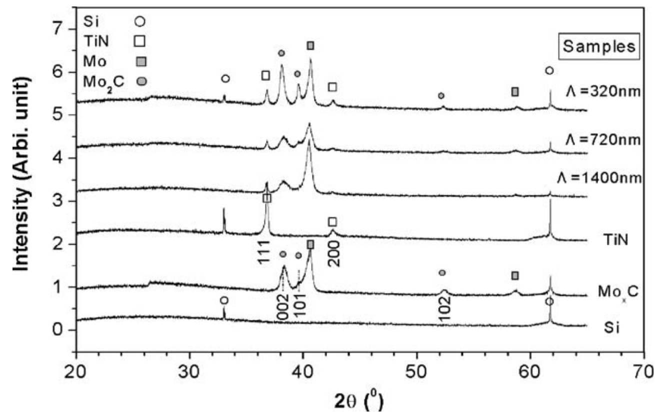

Fig. 1. The X-ray diffraction patterns for all films on the silicon substrate. Samples 12L, 6L, and 4L are multilayer films at a modulation period of 320, 720, and 1400 nm, respectively. The data for silicon substrate is also shown for comparison.

Table 1
Grain size (nm) of TiN, Mo_2C, and Mo phases in single layer films and multilayer films with various modulation periods

	Single layer	Λ = 1400 nm	Λ = 720 nm	Λ = 320 nm
TiN	90 ± 10	84 ± 10	110 ± 10	57 ± 10
Mo_2C	17 ± 5	12 ± 5	14 ± 5	26 ± 5
Mo	21 ± 5	21 ± 5	20 ± 5	35 ± 5

at 300 °C [18], implies that all the carbon would exist in Mo_2C crystallite. Because crystalline TiN phase can be formed at lower temperature with aid of plasma energy [20,21] and the proportion of Ti and N content is obtained as 1:1 from the EDS measurement, one could conclude that the Ti and N appear as the TiN crystallite.

In the multilayer films all three phases (TiN, Mo_2C, and Mo) explicitly show their diffraction peaks at the corresponding positions, as shown in Fig. 1. The grain size of the TiN, Mo_2C, and Mo phases in the multilayer films is almost same with that in the corresponding monolayer films when the modulation periods Λ are 1400 and 720 nm, as listed in Table 1. At Λ = 320 nm, however, the grain size of TiN seems to decrease to about 60 nm and that of the Mo_2C and Mo phases increases to 26 and 35 nm, respectively.

The FESEM images of the TiN/Mo_xC multilayer films at three different modulation periods Λ (320, 720, and 1400 nm), TiN and Mo_xC monolayer films are shown in Fig. 2. It can be seen clearly that the multilayer films form a finely modulated structure with straight and sharp interfaces. The total thickness of all films is about 2 μm and the thickness ratio between Mo_xC layer and TiN layer in the multilayer films is about 3:2. In the TiN monolayer film (Fig. 2a) the upper part displays clearly the coarse columnar grains in width of about 200 nm from the cross-section morphology, while the lower part close to the substrate is compact where columnar structure disappears due to the mismatch of crystal lattice between Si and TiN. This influence of lattice mismatch would decline with increasing deposition thickness and the crystallites grow more and more larger, and as a result the columnar structures appear after the thickness exceeds 800 nm. The monolayer Mo_xC film is relatively compact and does not exhibit columnar structure (Fig. 2b). In the multilayer films, however, where the largest thickness of TiN layers is about 500 nm, the size of columnar grains in TiN layers becomes smaller or even disappears (Fig. 2c–e), owing to the periodical introduction of Mo_xC layers that force the TiN crystallites to renucleate. In the Mo_xC films, the metallic phase of Mo suppresses the further growth of Mo_2C crystallites and the small size of Mo_2C and Mo crystallites also implies that a process of re-nucleation was dominating over continuous crystallite growth, similar to the case in TiN/a-C multilayer films [22].

3.2. Hardness measurement

The corresponding load–displacement curves for the Λ = 320 nm film were shown in Fig. 3, which shows a strong toughness behavior. It is obvious that the value of plastic length (the depth at unloaded state) versus the total indentation depth can reach as high as 60% that many ordinary ceramic materials cannot match with. It is worth noting

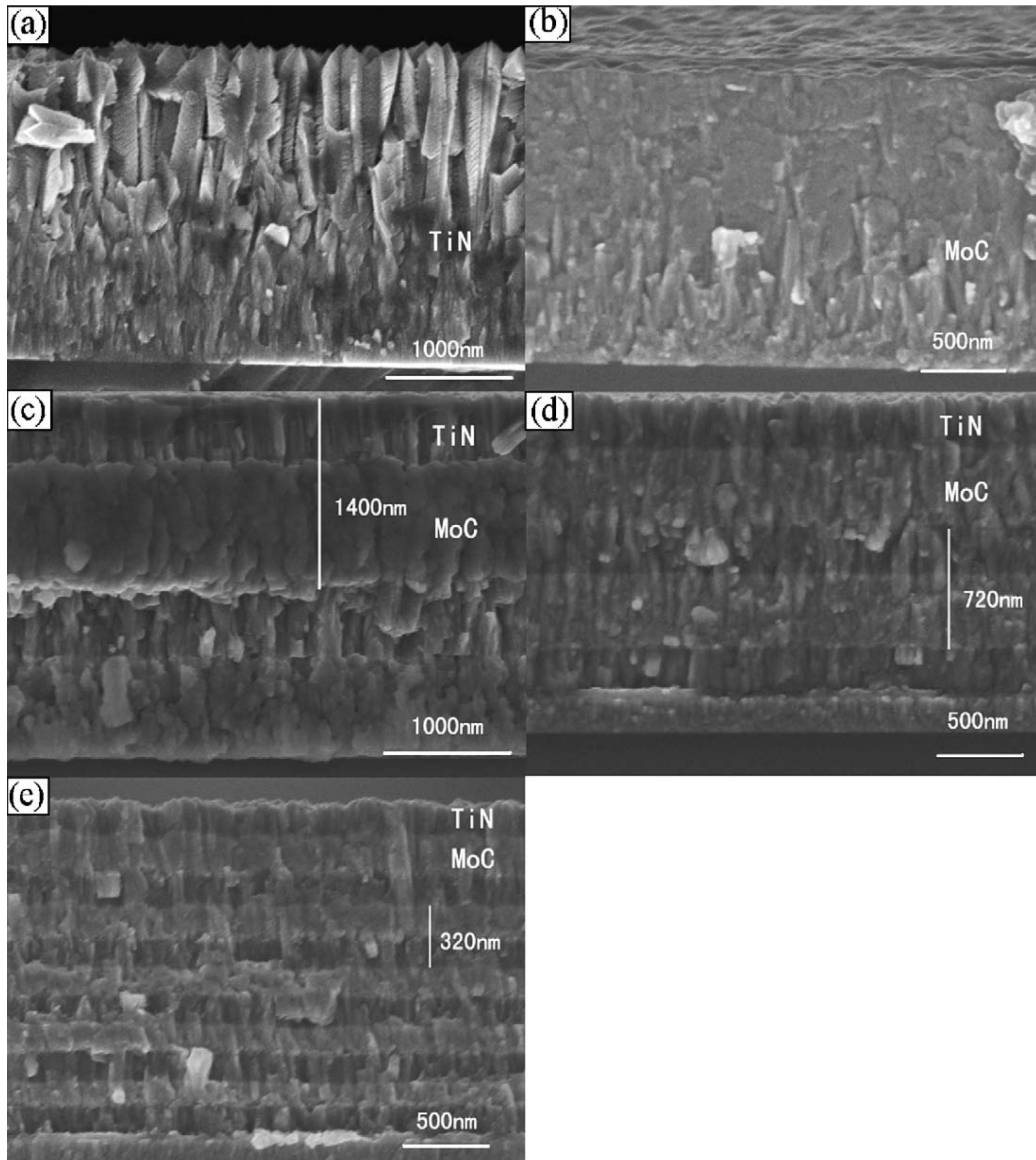

Fig. 2. FESEM cross-section micrographs of TiN/Mo_xC multilayer films and Mo_xC and TiN monolayer films: (a) 12-layer film (Λ = 320 nm); (b) 6-layer film (Λ = 720 nm); (c) 4-layer film (Λ = 1400 nm); (d) Mo_xC monolayer film; (e) TiN single-layer film.

that the maximum indentation depth at a load of 20 mN is about 220 nm, which is even smaller than the smallest value of Λ used in this paper.

Fig. 4 shows the hardness of all films as a function of modulation period Λ, where each point represents an average of 15 indentation measurements at three given loads (5, 10, and 20 mN). The TiN monolayer film has a hardness of 10 GPa owing to the columnar structure, which is similar to the value in PECVD deposited TiN film [23], but much lower than the usual values of 14–24 GPa depending upon the deposition conditions and the structure of the films [15,17,24]. The Mo_xC monolayer film has a hardness of 21 GPa. The hardness of the multilayer films increases with decreasing modulation period, and reach to a hardness of 26 GPa at Λ = 320 nm, which is higher than the hardness of both TiN and Mo_xC monolayer films. Chen et al. [15] have reported that the hardness of the TiN/SiN_x multilayer film with distinct layers and an equiaxed grain structure but no evidence of columnar growth is approximately twice that of TiN monolayer film. So the decrease in the columnar grain size

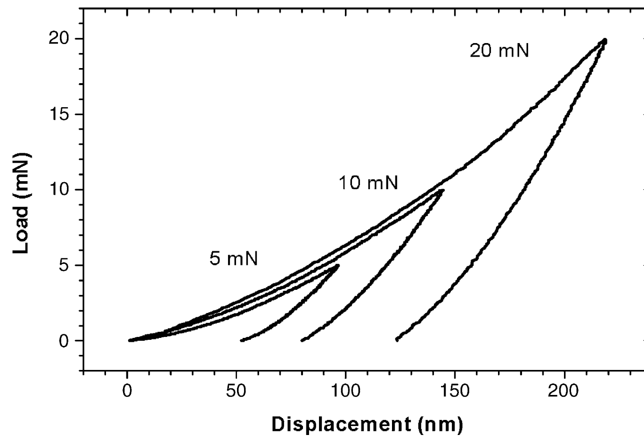

Fig. 3. Typical nanoindentation data for the TiN/Mo_xC multilayer film at Λ = 320 nm at different loads (5, 10, and 20 mN).

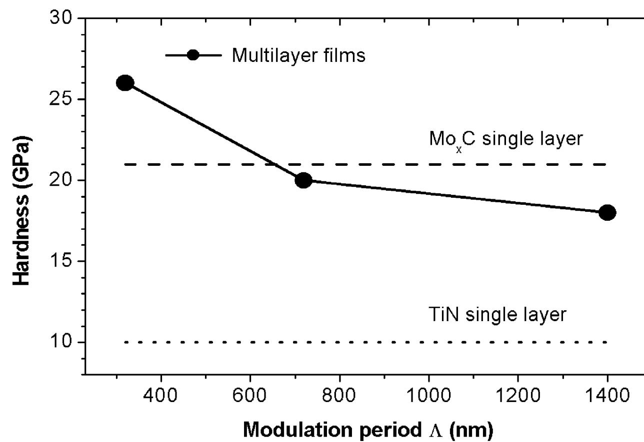

Fig. 4. The hardness as a function of modulation period Λ for TiN/Mo_xC multilayer films (points) and for Mo_xC and TiN monolayer films (lines).

seems to be one of the most important factors for the hardness enhancement in the multilayer films, especially in the case of large modulation period ($\Lambda > 100$ nm). Even at Λ = 1400 nm where the upper layer is TiN with a thickness of about 550 nm, the hardness of the multilayer films is much higher than that of TiN monolayer film. This fact indicates again the great influence of decrease in columnar grain size on the hardness because the deepest indentation depth is about 220 nm at 20 mN and the second upper layer of Mo_xC will have less contribution to the hardness. If the modulation period is lower than 320 nm as in the superlattice of transition-metal nitride, the hardness enhancement will be more remarkable as other researcher reported [5,25,26].

3.3. Young's modulus

The temperature dependence of the Young's modulus of films and a typical internal friction curve of a multilayer film at Λ = 320 nm, which have been deposited symmetrically on both sides of the molybdenum sheet with a total thickness of about 4 μm, is shown in Fig. 5. It was found that with decreasing modulation period in the range of 1400–320 nm, the Young's modulus of films increases monotonously from 340 to 430 GPa, similar to the value in magnetron sputtered TiSiN films measured with ultrasonic wave method [27]. The Young's modulus of the multilayer film at Λ = 320 nm has an anomaly enhancement compared with the other films, which is accordant with the hardness enhancement behavior. In the temperature range from 100 to 400 °C the Young's modulus of films decreases slightly

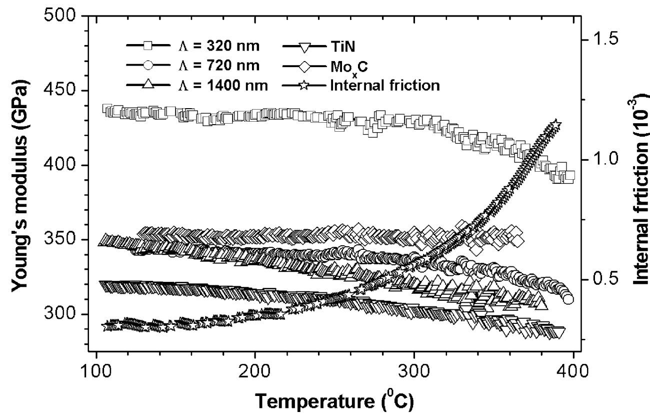

Fig. 5. The temperature dependence of the Young's modulus for all films on the Mo substrate and of the internal friction for the TiN/Mo_xC multilayer film at $\Lambda = 320$ nm.

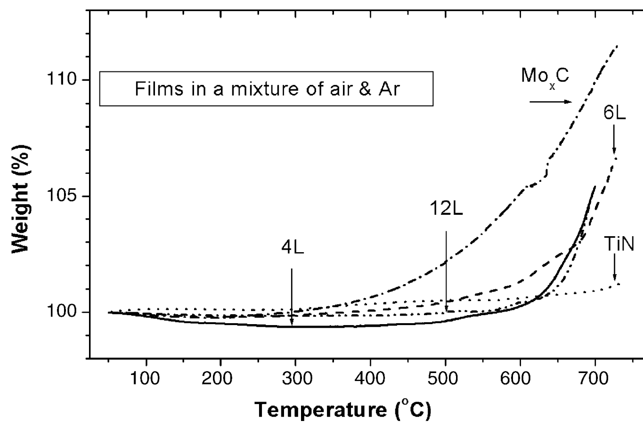

Fig. 6. Results of TGA for TiN/Mo_xC multiplayer films and for TiN and Mo_xC monolayer films.

and the internal friction of the films in the order of 10^{-3} increases monotonously with increasing temperature. Again it is expected that a greater enhancement of elastic modulus in the multilayer films would occur if $\Lambda < 320$ nm.

3.4. Oxidation resistance

Fig. 6 shows the results of TGA of all films obtained in a mixture of air and argon during a heating process. The small weight loss appeared at temperatures below 300 °C is due to the evaporation of moisture absorbed in the surface of films. From the figure we can see that the temperature at which the weight of the films starts to dramatically increase is about 400 °C for Mo_xC monolayer films. This temperature for TiN monolayer films is above 700 °C, in good agreement with the value reported in literature [28]. The weight of the multilayer films starts to increase over 600 °C insensitive to the modulation period, which implies that the oxidation resistance of multilayer films has been improved greatly owing to the protection of TiN layers.

4. Conclusion

The TiN/Mo_xC multilayer films at different modulation period Λ from 320 to 1400 nm have been deposited by magnetron sputtering. The TiN layer has a face-center cubic TiN phase, while the Mo_xC has a mixture of body-center cubic Mo phase and hexagonal Mo_2C phase. The hardness and Young's modulus of the multilayer films increase with decreasing Λ and the highest hardness and Young's modulus are obtained as 26 and 430 GPa at $\Lambda = 320$ nm.

The enhancement in hardness and Young's modulus of multilayer films could be understood as the decrease in the columnar grain size or disappearance of columnar structure in general. However, it looks like that the multilayer structure itself (not only the microstructure of the layers in the multilayer) also has some effect to the enhancement of the harness and Young's modulus, because the average grain sizes of the multilayer films are similar between modulation periods of 720 and 1400 nm but their hardness and Young's modulus were shown difference. The multilayer films show a much higher oxidation resistance than Mo_xC monolayer films owing to the protection of TiN layers.

Acknowledgement

This work has been subsidized by the National Natural Science Foundation of China (Grant No. 10274086).

References

[1] P. Panjan, B. Navinsek, A. Cvelbar, A. Zalar, I. Milosev, Thin Solid Films 298 (1996) 281.
[2] D.G. Kim, T.Y. Seong, Y.J. Baik, Thin Solid Films 397 (2001) 203.
[3] K. Kawata, H. Sugimura, O. Takai, Thin Solid Films 390 (2001) 64.
[4] Y.L. Su, W.H. Kao, Wear 223 (1998) 119.
[5] Y. Zhou, R. Asaki, W.H. Soe, R. Yamamoto, R. Chen, A. Iwabuchi, Wear 236 (1999) 159.
[6] J.D. Embury, J.P. Hirth, Acta Metall. Mater. 42 (1994) 2051.
[7] P.M. Anderson, C. Li, Nanostruct. Mater. 5 (1995) 349.
[8] Helmersson, S. Todorova, S.A. Barnett, J.E. Sundgren, J. Appl. Phys. 62 (1987) 481.
[9] M. Shinn, L. Hultman, S.A. Barnett, J. Mater. Res. 7 (1992) 901.
[10] P.B. Mirkarimi, S.A. Barnett, Appl. Phys. Lett. 57 (1990) 2654.
[11] J.S. Koehler, Phys. Rev. B 2 (1970) 547.
[12] X. Chu, S.A. Barnett, J. Appl. Phys. 77 (1995) 4403.
[13] I.A. Polonsky, T.P. Chang, L.M. Keer, W.D. Sproul, Wear 208 (1997) 204;
I.A. Polonsky, T.P. Chang, L.M. Keer, W.D. Sproul, Wear 215 (1998) 191.
[14] S. Veprek, M.G.J. Veprek-Heijman, P. Karvankova, J. Prochazka, Thin Solid Films 476 (2005) 1.
[15] Y.H. Chen, K.W. Lee, Y.W. Chung, L.M. Keer, Surf. Coat. Technol. 146/147 (2001) 209.
[16] Q.F. Huang, S.F. Yoon, Rusli, H. Yang, J. Ahn, Q. Zhang, Diam. Relat. Mater. 9 (2000) 534.
[17] J. Kozlowski, J. Markowski, A. Prajzner, J. Zdanowski, Surf. Coat. Technol. 98 (1998) 1440.
[18] Q. Liu, T. Liu, Q.F. Fang, F.J. Liang, J.X. Wang, Thin Solid Films 503 (2006) 79.
[19] Z.S. Li, Q.F. Fang, S. Veprek, S.Z. Li, Mater. Sci. Eng. A 370 (2004) 186.
[20] M. Diserens, J. Patscheider, F. Levy, Surf. Coat. Technol. 108/109 (1998) 241.
[21] S. Veprek, J. Vac. Sci. Technol. A 17 (1999) 2401.
[22] A.A. Voevodin, S.V. Prasad, J.S. Zabinski, J. Appl. Phys. 82 (1997) 85.
[23] T.H. Fang, S.R. Jian, D.S. Chuu, Appl. Surf. Sci. 228 (2004) 365.
[24] C.H. Ma, J.H. Huang, H. Chen, Surf. Coat. Technol. 200 (2006) 3868.
[25] J. Xu, M. Kamiko, Y. Zhou, R. Yamamoto, J. Appl. Phys. 89 (2001) 3674.
[26] J.L. He, W.Z. Li, H.D. Li, Mater. Lett. 30 (1997) 15.
[27] F. Vaz, S. Carvalho, L. Rebouta, M.Z. Silva, A. Paul, D. Schneider, Thin Solid Films 408 (2002) 160.
[28] D.Y. Wang, M.C. Chiu, Surf. Coat. Technol. 156 (2002) 201.